Vortex Subdomains

KARL GUSTAFSON* AND ROBERT LEBEN†

Abstract. The physical problem of the formation and evolution of vortices in fluids is of great scientific interest. Vortices are known to form and occur in corners and near separation points. Because the problem is biharmonic, even the motion of a slow (Stokes, linearized) viscous incompressible fluid in a corner cannot be solved analytically.

Mathematical asymptotics and physical experiments indicate the existence of a sequence, possibly infinite, of vortices descending into a corner. By a multigrid nested subdomain scheme we have resolved twenty of these. This scheme has then been adapted to unsteady flow over an airfoil. Examples and numerical considerations will be given and discussed.

Fluid Dynamics and its mathematical description in terms of the Navier-Stokes equations are fundamental in theoretical and applied sciences including physics, aerodynamics, meteorology, oceanography and other basic sciences. In particular the physical problem of the formation and evolution of vortices in fluids is of great scientific interest. Its relation to dynamical instability led Lewis Richardson in his prophetic book [1] to the renowned

> big whirls have little whirls that feed on their velocity,
> and little whirls have lesser whirls and so on to viscosity.

Richardson was describing cloud motions and goes on

> because it is not possible to separate eddies into clearly defined classes ... therefore a single coefficient is used to represent the effect produced by eddies of all sizes.

* Department of Mathematics, University of Colorado, Boulder, CO 80309.
† Department of Aerospace Sciences, University of Colorado, Boulder CO 80309.

Earlier, Lord Rayleigh [2] attacked the problem mathematically, attempting the analysis of the motion of a viscous incompressible fluid in a corner:

> The general problem thus represented is one of great difficulty, and all that will be attempted here is the consideration of one or two particular cases. We inquire what solutions are possible such that ψ, as a function of r (the radius vector), is proportional to r^m.

Even with his assumption of slow motion (Stokes) linearized equations, Rayleigh was unable to fit the boundary conditions with his proposed solutions. The fact that this (biharmonic) linear problem on a square still cannot be solved exactly has to be an embarrassment to those of us working in fluids theory or in plate theory where it also occurs.

Eventually, from ideas in plate theory, a series of papers led to that of Moffatt [3], which under serious simplifying assumptions predicted an infinite sequence of standing vortices descending into a corner of sufficiently small angle. Some of these have been verified, e.g., up to a third corner vortex, in recent physical experiments, Taneda [4], Fuchs and Tillmark [5]. Because these corner subvortices drop in intensity like $O(10^{-4})$, practioners of Stokes flow may not see them and in some case we have found that practioners do not even believe in their existence!. Certainly the question of how many of them *really* persist within the fluid breakdown process portrayed by Lewis Richardson's verse is an intriguing one, with many ramifications physically, mathematically, computationally, perhaps philosophically, and certainly for important applications.

In order to investigate both the computational and applications aspects of this question of subvortex existence and structure, we developed a very robust multigrid nested subdomain scheme. This nested subdomain scheme applied to Stokes flow in a unit cavity is depicted in Figures 1 and 2. Convergence was excellent and we were able [6] to report ten corner subvortices, by far the best resolution reported to that date. These were obtained in a vectorized run on the Cyber 205 with a discretization of 129 by 129 points and 40 nested subdomains, in under 15 CPU seconds.

Our results in [6] were limited by machine precision (recall the rapid $O(10^{-4})$ subvortex intensity falloff), a glitch in the local 205 software that prevented efficient vectorized grid lengths finer than $(2^{16}-1)/2$, and a rapid buildup in the number of iterations needed as the subdomain size decreased as we nested down into the corner. By using double precision accurate, residual-controlled code we can now report resolution of twenty corner subvortices.

The results for two grid discretizations M are shown in Table 1. The number of grid poin.ts on a side of the computational domain is given by $NP = 2^M + 1$ Our algorithm employed an adaptive iteration strategy which maintained the residual defined by:

$$\text{Residual} = |\nabla^2\psi + \omega| + |\nabla^2\omega|$$

below a pointwise tolerance of 10^{-4}. The number of iterations required increased as the localization procedure progressed.

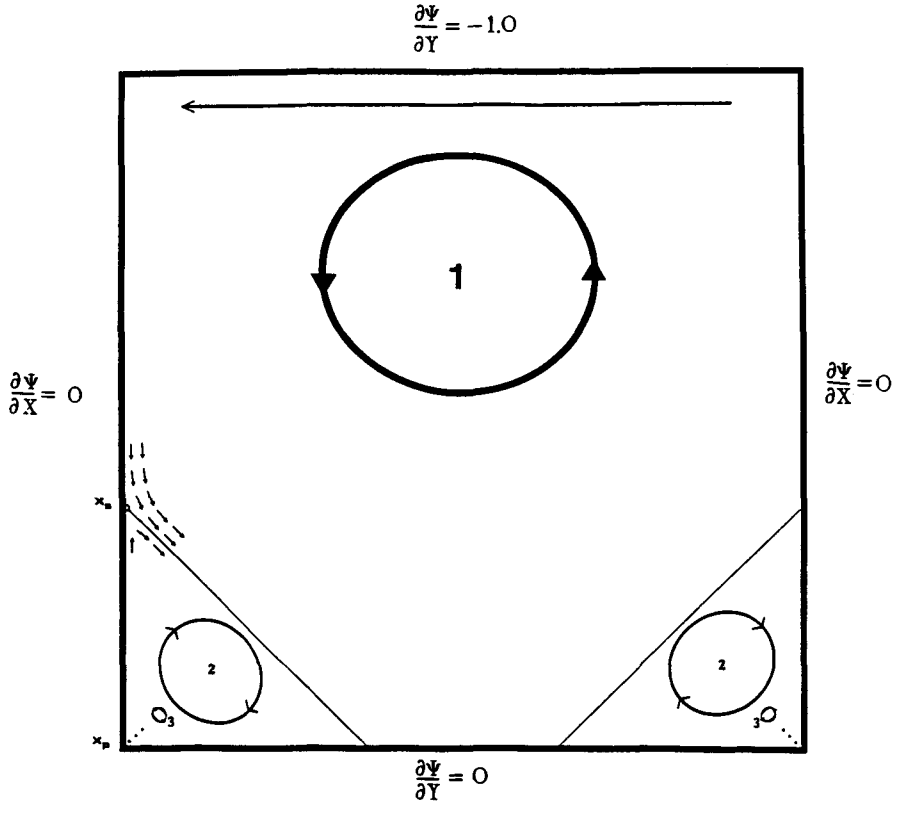

Figure 1. Driven Cavity Flow, A = 1.

1: Principal Vortex
2: Secondary Corner Vortex
3: Tertiary Corner Vortex
x_s: Separation Point
x_p: Provocation point

Note from Table 1 that the subvortices occur in a (essentially, self-similar) sequence of subdomains of shrinking scale close to 2^{-4}. One could take this into account in assigning the nested subdomain decomposition. Our scheme simply halved the domain size and then reapplied our residual-controlled multigrid scheme. Thus we encountered a new vortex subdomain after (roughly) each four localizations.

Our present scheme does not yet employ any back and forth local-global subdomain interaction. This no doubt accounts for most of our difficulty in maintaining accuracy on the subdomains. Because the problem is basically biharmonic, the analytic theory of these vortex subdomains is also, generally speaking, quite lacunate on this point. Further research on appropriate boundary values, optimal grid transfer stencils, parallel subdomain processing, and needed domain decomposition overlap would be important.

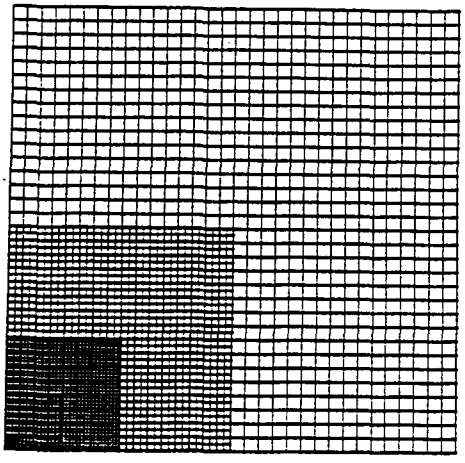

Figure 2(b). Grid hierarchy for resolution of Moffatt vortices.

Figure 2(c). Grid hierarchy for resolution of separation point, x_s .

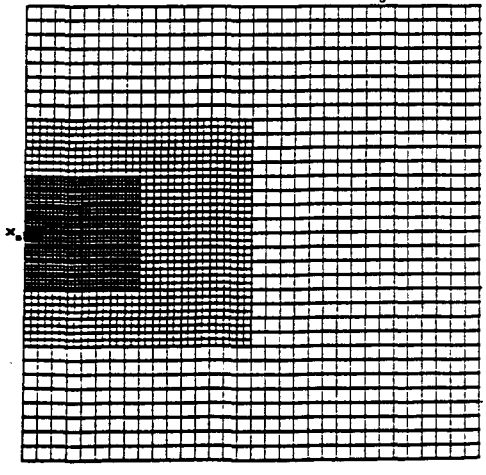

Figure 2(a) Interpolation Procedure

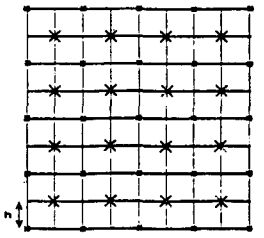

x: Injected red grid points.

X: Remaining red grid points interpolated using rotated difference equation.

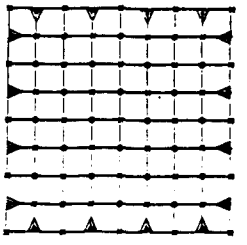

x: Red grid points

o: Interpolated black grid points

A: Interpolated boundary points

Boundary Interpolation Stencils:

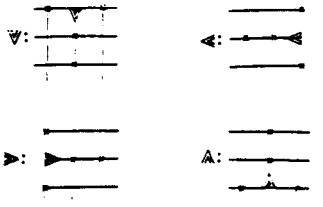

Figure 2. Nested Domain Decomposition

To be more precise, the following algorithm should be investigated. Thinking first in terms of the simpler Poisson Problem $Lu = f$ where L denotes the Laplacian operator on a convenient domain, e.g., first the unit square, assuming that one has a nested domain decomposition such as that of Figure 2, and assuming that one has global and local solutions u_g and u_l respectively, the data flow of our proposed local to global interaction algorithm is:

$$
\begin{array}{lllll}
\text{(local)} & u_l \rightarrow r_l = f - Lu_l & u_{cl} = I_g^l u_{cf} \rightarrow u_l = u_l + u_{cl} & & \text{(local)} \\
 & \downarrow & \uparrow & & \\
 & r_{lg} = I_l^g r_l \rightarrow L_g v = f_g + r_{lg} & & & \\
\text{(global)} & r_{lg} = 0 \quad \begin{array}{c}\text{on non}\\ \text{member}\\ \text{grid points}\end{array} & u_{cf} = v - u_g & & \text{(global)}
\end{array}
$$

For the biharmonic equations of the fluid corner subdomains one would have a similar scheme although a number of interesting new domain decomposition questions concerning information exchange already arise:

(i) Can we seek corrections to ω and ψ simultaneously? Recall that there is a strong coupling between the ψ and ω equations because the boundary conditions on the vortices ω depend on interior stream function values of ψ.

(ii) Need we correct just boundary points ($\sim$ FAC), or also some or all interior points, and how may we transfer the data to them most efficiently? In particular, in a parallel processing environment such as the hypercube, how do we optimally allocate the computations?

TABLE 1

Local Maximum Stream Function Intensities

	M = 5	M = 6
ψ_1	0.996×10^{-1}	0.10002
ψ_2	-2.29×10^{-6}	-2.24×10^{-6}
ψ_3	6.55×10^{-11}	6.24×10^{-11}
ψ_4	-1.87×10^{-15}	-1.73×10^{-15}
ψ_5	5.33×10^{-20}	4.83×10^{-20}
ψ_6	-1.52×10^{-24}	-1.34×10^{-24}
ψ_7	4.34×10^{-29}	3.73×10^{-29}
ψ_8	-1.24×10^{-33}	-1.04×10^{-33}
ψ_9	3.53×10^{-38}	2.88×10^{-38}
ψ_{10}	-1.01×10^{-42}	-0.80×10^{-42}
ψ_{11}	2.88×10^{-47}	2.23×10^{-47}
ψ_{12}	-8.19×10^{-52}	-6.21×10^{-52}
ψ_{13}	2.34×10^{-56}	1.73×10^{-56}
ψ_{14}	-6.69×10^{-61}	-4.81×10^{-61}
ψ_{15}	1.91×10^{-65}	1.34×10^{-65}
ψ_{16}	-5.45×10^{-70}	-3.72×10^{-70}
ψ_{17}	1.55×10^{-74}	1.03×10^{-74}
ψ_{18}	-4.42×10^{-79}	-2.88×10^{-79}
ψ_{19}	1.27×10^{-83}	8.00×10^{-84}
ψ_{20}	-3.61×10^{-88}	-2.22×10^{-88}
ψ_{21}	1.03×10^{-92}	6.18×10^{-93}

(iii) What are the trade-offs between fully overlapped processing (e.g., keeping each CPU fully occupied) and best parallelism in information passing?

Improved knowledge gained from the investigation of this algorithm would be invaluable in application to other important geometries exhibiting subvortical subdomain structures. A particularly important one is flow about an airfoil, to which we return below.

To fully understand subvortex generation and their subsequent dynamical evolution brings one to the full nonlinear *unsteady* Navier-Stokes equations and to one of the most important and fundamental problems in Fluid Dynamics, namely, boundary layer separation. Such subvortex sequences appear to be initiated by a sublayer viscous-inviscid bursting effect at a wall separation point. In recent numerical experiments in a cavity we have uncovered [7,8] a very rich subsequent dynamics, including vortex pairs exhibiting multiple fusions and fissions as they travel on their way to a final state. Some represent transient bifurcations whereas others, at sufficiently high Reynolds numbers, persist, indicating Hopf bifurcations in the steady equations.

Specifically, there appear [7,8] to be critical Reynolds numbers (related, so let us call them $Re_c(A)$ and $A_c(Re)$) and Aspect ratios A = depth/width somewhere in the range $2000 < Re < 10{,}000$, $1 < A < 2$ at which the final solutions are periodic rather than steady. Thus the conjecture of [9], that multiple steady solutions in a unit $(A = 1)$ cavity would not appear until $Re > 5000$, is perhaps better understood as the occurrence of final unsteady periodic solutions. See Figure 3. Our results in [7,8] show that going to aspect ratio A definitely greater than one is a parameter perhaps more important than greatly increasing Reynolds number. Our current work [10] strongly suggests that the occurrence of such solutions is very dependent on the nonlinearity in the equations, and even if missed on a too-coarse mesh, is fundamentally not really mesh dependent. How to preassign or adaptively assign subdomain decompositions appropriate to capture swirling, secondary, and even finer fluid structure detail such as that evident in Figure 3, raises many challenging domain decomposition considerations for problems of *unsteady* flow.

Many other important physical domains may be treated by the multigrid cavity scheme described above. In particular we may consider unsteady flow over an airfoil. In order to study this and other geometries, a numerical grid generation procedure must be employed. There are a large variety of grid generation techniques including partial differential equation methods, algebraic methods and conformal transformations. We selected an elliptic partial differential equation method which allows the construction of orthogonal coordinates on infinite domains. The selection of an elliptic generation technique was also motivated by the aim of our research, namely, the solution of the unsteady Navier-Stokes equations which govern unsteady flows in the laminar flow regime. The calculation of developing flow patterns governed by these equations requires that Poisson's equation be solved at each time step of the computation. The Poisson equation is by definition the generation equation for the coordinates of a grid system when elliptic grid generation techniques are used. Thus, efforts to make the solution of the generation equations more efficient also increases the efficiency of the Navier-Stokes solution procedure.

The problem of grid generation around airfoils also requires the use of a method allowing calculation of boundary-fitted coordinates. This simply means that the method must allow a prescribed distribution of coordinate nodes along the boundary of the grid, so that airfoil domains of a given shape can be generated. The most popular of such methods is the numerical technique of Thompson *et al.* [11] which allows the construction of a non-orthogonal, boundary-fitted coordinate system using elliptic

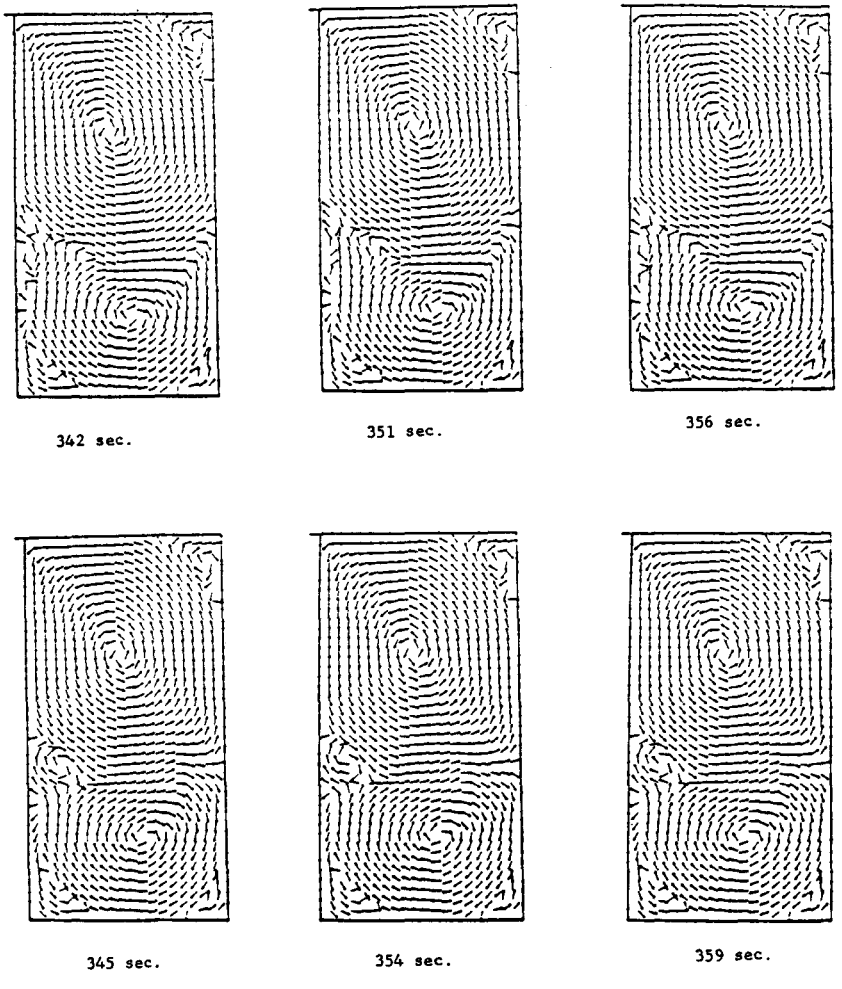

Figure 3. Final Oscillation at Re = 10,000, A = 2.

generation equations. While the non-orthogonality of the method is not a severe drawback, it does require more computational work than comparable orthogonal systems, due to the extra terms in the transformed partial differential equations which requires nine point stencil instead of the five point stencil used on orthogonal systems. Also, extreme non-orthogonality can effect the truncation error of a solution.

The grid generation technique of Ryskin and Leal [12] allows the construction of orthogonal boundary-fitted coordinate systems, when the weak constraint form of their method is employed. This method is relatively straight forward, yet quite robust. In addition, it includes a procedure for construction of infinite coordinate systems. Using this procedure the difficulties associated with outflow boundary conditions on conventional domains can be avoided.

The orthogonal grid generation equations, being elliptic, may of course be solved numerically by a variety of schemes. In [12] an ADI method was employed, whereas in

[13] an SOR scheme was used. Here we describe a Multigrid scheme [14] which, as mentioned above, also has the advantage of providing efficient solutions to the flow equations themselves. It has enabled [14] remarkable agreement with visualizations of physical flows about airfoils [15].

To describe this adaptation of the cavity multigrid solver scheme to flow about an airfoil, let us direct the reader to Figure 4. Briefly (more detail will be given in [14]), we first analytically map the exterior domain about the airfoil onto a more convenient interior domain. For the NACA 0015 airfoil, the domain boundary is given by

$$y = \pm \frac{t}{0.20}\left(0.2969X^{1/2} - 0.1260X - 0.3516X^2 + 0.2843X^3 + 0.1015X^4\right)$$

where $t = 0.15$. Under the inverse Joukowski map the boundary becomes nearly circular. This is advantageous in allowing us good initial guesses for the orthogonal grid coordinates x and y. The X and Y coordinates must in fact be shifted somewhat (see [13]) in the physical domain to provide the most circular-like image in the auxiliary domain.

We may then develop an orthogonal grid in the auxiliary domain by employing a multigrid elliptic solver based on the cavity computational domain. Following [12], the equations defining the mapping are

$$\frac{\partial}{\partial \xi}\left(f \frac{\partial x}{\partial \xi}\right) + \frac{\partial}{\partial \eta}\left(\frac{1}{f} \frac{\partial x}{\partial \eta}\right) = 0$$

$$\frac{\partial}{\partial \xi}\left(f \frac{\partial y}{\partial \xi}\right) + \frac{\partial}{\partial \eta}\left(\frac{1}{f} \frac{\partial y}{\partial \eta}\right) = 0$$

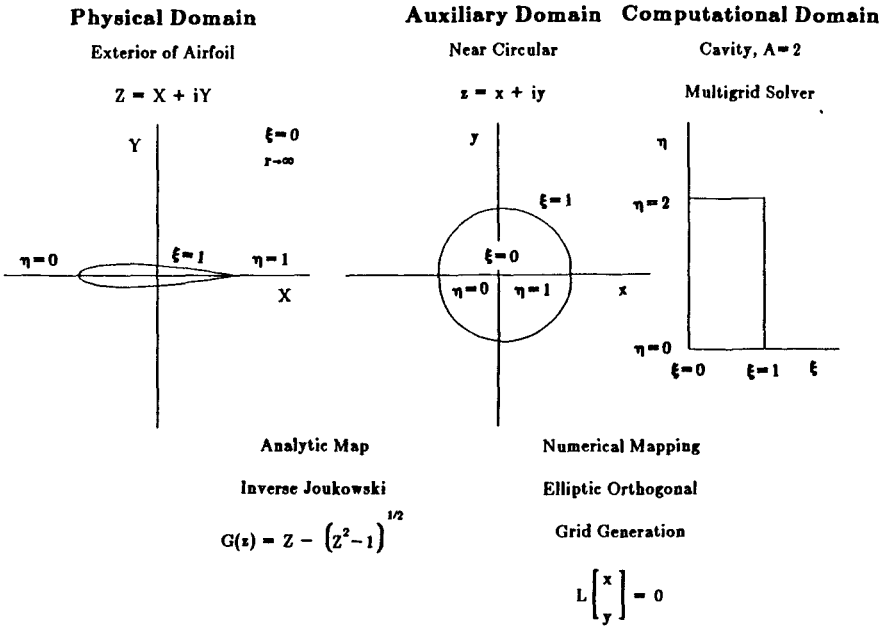

Figure 4. Multigrid Calculation of Boundary-Fitted Coordinates

where the distortion function is given by

$$f(\xi,\eta) = \frac{h_2}{h_1} = \frac{(x_\eta^2+y_\eta^2)^{1/4}}{(x_\xi^2+y_\xi^2)^{1/4}}$$

with h_1 and h_2 denoting the scale factors in the ξ and η directions, respectively. The distortion function specifies the ratio of the sides of a small rectangle in the auxiliary domain which is the image of a small square in the computational domain.

The mapping equations are discretized using second order accurate difference formulas. Stencil coefficients can be precalculated and stored for efficiency. The computational procedure for calculation of the orthogonal grid is then as follows. First, one makes initial guesses of x and y on the boundary of the computational cavity domain. These x, y values on the boundary of the cavity are then interpolated throughout this computational domain. From them (and their differences) the distortion function $f(\xi,\eta)$ may be found. It was more efficient to compute f just on the boundary and then interpolate (so-called weak constraint method) f to the interior. For this, formulae such as $f(\xi,\eta) = \xi f(1,\eta)$ may be used so that $f = 0$ at $\xi = 0$ which corresponds to the singularity at ∞ in the physical domain. Note that use of such a weak constraint does, however, affect the relaxation steps in the multigrid solution of the grid equations. Continuing, using these values of f in the elliptic mapping equations, the cavity multigrid solver with Dirichlet boundary conditions gives new values for $x(\xi,\eta)$, $y(\xi,\eta)$. An orthogonality check then determines whether another f, x, y iteration is needed.

Once an orthogonal grid is established by the above algorithm, one returns by inverse map

$$X = \frac{1}{2}\left(x + \frac{x}{r^2}\right), \quad Y = \frac{1}{2}\left(y - \frac{y}{r^2}\right)$$

from the auxiliary domain to the physical domain. The resultant physical grid is orthogonal. Figure 5 shows such a grid about an NACA 0015 airfoil, and the corresponding auxiliary domain and the computational cavity domain.

By use of appropriate boundary conditions for the stream function ψ and vorticity ω, full unsteady Navier-Stokes flow about an airfoil may be computed in the cavity and then returned by the above mappings to the physical domain. Space limitations prevent a full detailing of this procedure here, see [14]. Briefly, the Multigrid

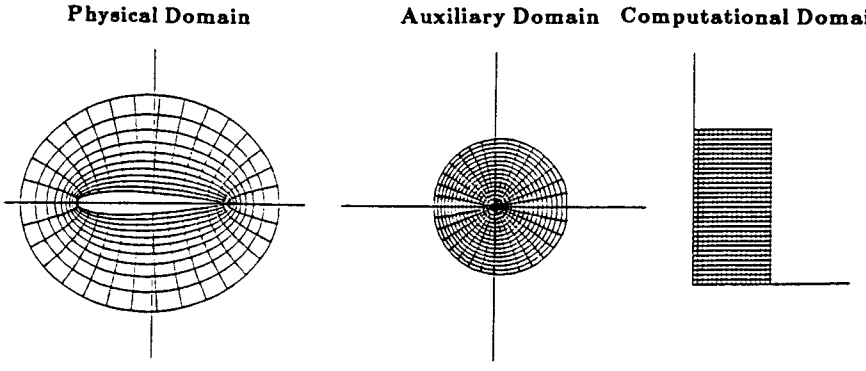

Figure 5. Numerically Generated Grids

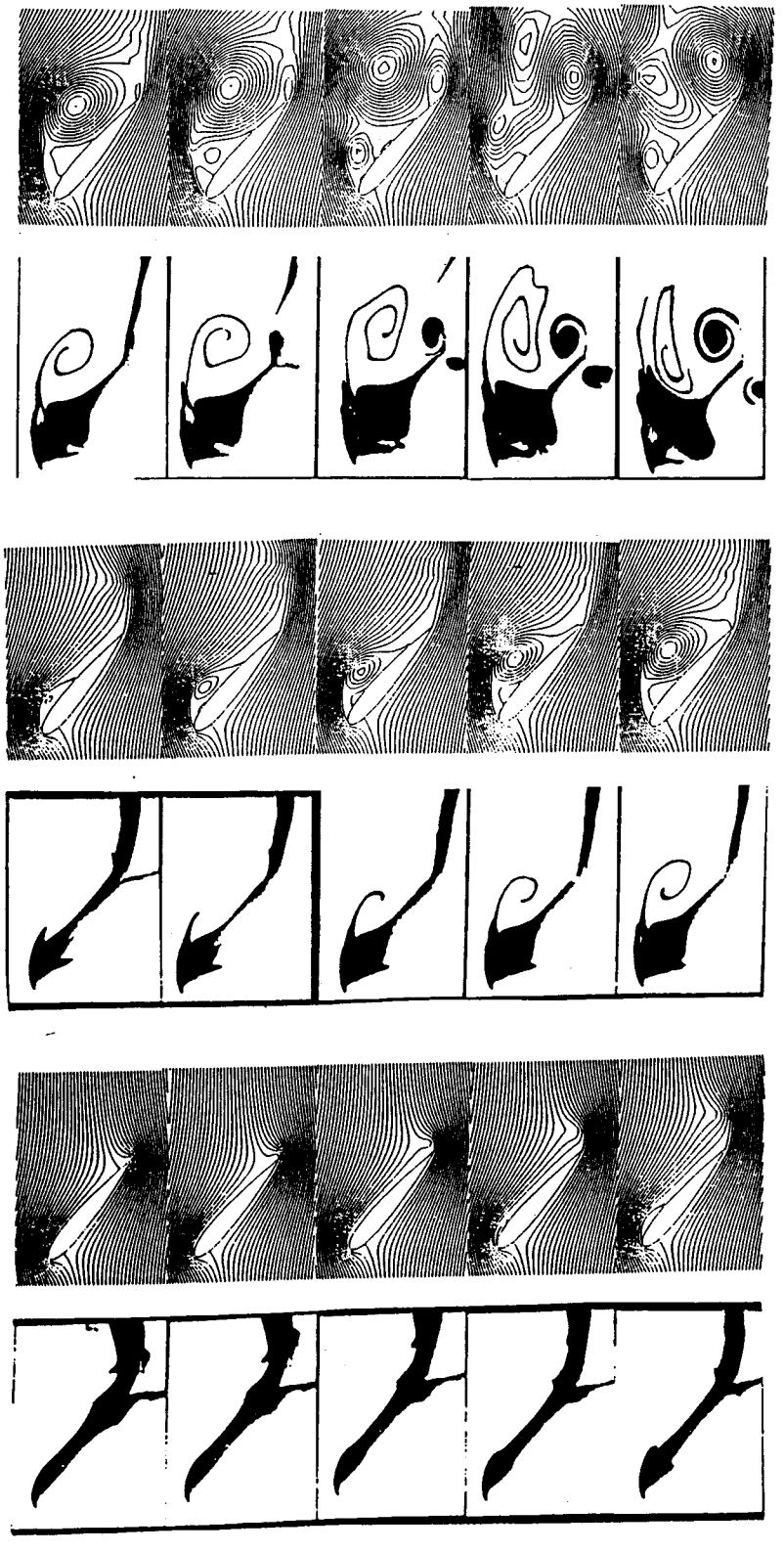

Figure 6. Experimental and Numerical Flows
Re = 1000 $\alpha = 40^{\circ}$

solver yields the stream function values, an ADI time-marching scheme enabled vorticity transport. Examples of the output follow, see Figure 6. Here an angle of attack $\alpha = 40$deg was simulated. Note that vortex splitting and the vortex subdomain structure near the airfoil is remarkably well resolved. The comparison is to physical simulations taken from [15].

REFERENCES

1. Lewis Richardson, "Weather Prediction by Numerical Process," Cambridge University Press (1922).
2. Lord Rayleigh, "On the question of the stability of the flow of fluids," *Phil. Magazine* 34 (1892), 59-70.
3. H. Moffatt, "Viscous and resistive eddies near a sharp corner," *J. Fluid Mech.* 18 (1964), 1-18.
4. S. Taneda, "Visualization of separating Stokes flows," *J. Phys. Soc. Japan* 46 (1979), 1935-1942.
5. L. Fuchs and N. Tillmark, "Numerical and experimental study of driven flow in a polar cavity," *International J. Num. Meth. in Fluids* 5 (1985), 311-329.
6. K. Gustafson and R. Leben, "Multigrid calculation of subvortices," *Applied Math. and Computation* 19 (1986), 89-102.
7. K. Gustafson and K. Halasi, "Vortex dynamics of cavity flows," *J. Computational Physics* 64 (1986), 279-319.
8. K. Gustafson and K. Halasi, "Cavity flow dynamics at higher Reynolds number and higher aspect ratio," *J. Computational Physics* 70 (1987), 271-283.
9. R. Glowinski, H. Keller, L. Reinhart, "Continuation-conjugate gradient methods for the least squares solution of nonlinear boundary value problems," *SIAM J. Sci. Stat. Computing* 6 (1985), 793-832.
10. K. Gustafson and R. Leben, to appear.
11. J.F. Thompson, Z.U.A. Warsi, and C.W. Mastin, "Numerical Grid Generation," Elsevier Science Publishing (1985).
12. G. Ryskin and L.G. Leal, "Orthogonal mapping," *J. Computational Physics* 50 (1983), 71-100.
13. E.D. Chikhliwala and Y.C. Yortsos, "Application of orthogonal mapping to some two-dimensional domains," *J. Computational Physics* 57 (1985), 391-402.
14. C.Y. Chow, K. Gustafson, R. Leben, to appear.
15. P. Freymuth, "The vortex patterns of dynamic separation: a parametric and comparative study," *Prog. Aerospace Sciences* 22 (1985), 161-208.